

Evaluating the accuracy of gridded water resources reanalysis and evapotranspiration products for assessing water security in poorly gauged basins

Elias Nkiaka¹, Robert G. Bryant¹, Joshua Ntajal^{2,3}, Eliezer I. Biao⁴

¹Department of Geography, University of Sheffield, Sheffield, S10 2TN, UK

²Department of Geography, University of Bonn, 53115 Bonn, Germany

³Center for Development Research, University of Bonn, 53113 Bonn, Germany

⁴Laboratory of Applied Hydrology, University of Abomey-Calavi (UAC), Cotonou, Benin

Elias Nkiaka (Corresponding author): e.nkiaka@sheffield.ac.uk

Postal Address: Department of Geography, University of Sheffield, Sheffield, S10 2TN, UK

Abstract

Achieving water security in poorly gauged basins is critically hindered by a lack of in situ river discharge data to assess past, current and future evolution of water resources. To overcome this challenge, there has been a shift toward the use of freely available satellite and reanalysis data products. However, due to inherent bias and uncertainty, these secondary sources require careful evaluation to ascertain their performance before being applied in poorly gauged basins. The objectives of this study were to evaluate river discharge and evapotranspiration estimates from eight gridded water resources reanalysis (WRR), six satellite-based evapotranspiration (ET) products and ET estimates derived from complimentary relationship (CR-ET) across eight river basins located in Central-West Africa. We also estimated the relative uncertainties in monthly basin-scale water balance evapotranspiration (ET_{WB}) across all the basins. Results highlight strengths and weaknesses of the different WRR in simulating discharge dynamics and ET across the basins. Likewise satellite-based products also show some strength and weaknesses in simulating monthly ET. Analyses further revealed that the relative uncertainties in monthly ET_{WB} range from 4–25 % with a significant increase in magnitude during the rainy season while river discharge appear to be the dominant source of uncertainty. Our results further revealed that the performance of the models in simulating river discharge and evapotranspiration is strongly influenced by model structure, input data and spatial resolution. Considering all the evaluation criteria Noah, Lisflood, AWRAL, and Terra are among the best performing WRR products while Noah, Terra, GLEAM3.5a & 3.5b, and PMLV2 produced ET estimates with the least bias. Given the plethora of WRR and ET products available, it is imperative to evaluate their performance in representative gauged basins to identify products that can be applied in each region. However, the choice of a particular product will depend on the application and users requirements. Results from this study suggest that gridded WRR and ET products are a useful source of data for assessing water security in poorly gauged basins.

34 **1. Introduction**

35 River discharge is one of the most important hydrological variables underpinning water resources
36 management, aquatic ecosystems sustainability, flood prediction, and drought warnings at different
37 scales (McNally et al., 2017; Couasnon et al., 2020). However, observed river discharge data is often
38 not available at the exact location where critical water management decisions need to be made (Neal
39 et al., 2009). This is especially the case in developing and semi arid/arid regions where discharge
40 gauging stations are sparse (Krabbenhof et al., 2022), while the number of existing stations are
41 declining (Rodríguez et al., 2020). Despite the acute shortage in observed data, developing regions
42 are areas that are more vulnerable to adverse hydroclimatological conditions (Byers et al., 2018;
43 Kabuya et al., 2020). Furthermore, achieving water security in poorly gauged basins remains a critical
44 development challenge as climate change, population growth, rapid urbanization, and economic
45 growth continue to exert pressure on available water resources under hydrological uncertainty (Flörke
46 et al., 2018; Hirpa et al., 2019). This highlights the urgent need for more reliable data to better assess
47 past, current, and future evolution of water resources, and to predict extreme hydroclimatological
48 events so that better strategies can be put in place to enhance water management and mitigate the
49 impact of extreme events (Nkiaka et al., 2020; Slater et al., 2021). Water security in this study refers
50 to the availability of sufficient quantities of water for human use and ecosystem sustainability.

51 Evapotranspiration (ET) is another important hydrological variable that represents the linkage
52 between water, energy and carbon cycles and ecosystem services and is the second largest process in
53 the hydrological cycle after precipitation (Zhang et al., 2019). Therefore, ET plays a critical role in
54 water availability at different scales. As such, accurate estimates of ET are also crucial for water
55 management operations such as basin-scale water balance estimation, irrigation planning, estimating
56 water footprint, and assessing the impact of climate change on water availability. However, globally,
57 in situ ET monitoring stations are also scarce while the existing monitoring network cannot provide
58 sufficient information on the temporal and spatial trends of ET at large scales (Laipelt et al., 2021).
59 ET data scarcity may therefore limit our ability to understand changes in the hydrological cycle and
60 water security in the context of environmental change and hydrological uncertainty.

61 To enhance water security in poorly gauged basins, there has been a progressive shift toward
62 the use of gridded data derived from satellite and reanalysis (Odusanya et al., 2019; Nkiaka, 2022).
63 This is because gridded data products can provide high spatial resolution and long-term homogeneous
64 data for previously unmonitored areas at scales that are suitable for studying changes in the
65 hydrological cycle and for water management applications (Sheffield et al., 2018). Several gridded
66 data products with global coverage have been produced in recent decades including reanalysis and
67 satellite-based products. Examples of reanalysis products include Watch Forcing Data applied to
68 ERA-Interim (Weedon et al., 2014) and Climate Forecast System Reanalysis (Saha et al., 2014).

69 There is also a plethora of satellite products for different hydrometeorological variables such as
70 precipitation, temperature, soil moisture, and ET. For satellite derived ET estimates, it is worth noting
71 that this variable cannot be directly measured by satellites, but rather derived from physical variables
72 observed by satellites from space such as radiation flux. As such, satellite derived ET estimates could
73 rather be referred to as model outputs constrained by satellite data. Another technique used to produce
74 ET estimates is the complimentary relationship (Ma et al., 2021). Considering the way gridded ET
75 products are derived, they tend to suffer from large biases (Weerasinghe et al., 2020; Mcnamara et
76 al., 2021) and therefore need to be validated before use. In fact, it is argued that validating gridded
77 ET products is an essential step in understanding their applicability and usefulness in water
78 management operations (Blatchford et al., 2020).

79 Previously, much attention in the development of gridded environmental data was focused on
80 hydrometeorological variables such as precipitation and temperature. However, rapid advancement
81 in computer technology has led to the development of gridded water resources reanalysis (WRR) with
82 quasi global coverage using both land surface models (LSMs) and Global Hydrological Models
83 (GHMs) driven by satellite and reanalysis data. Examples of WRR products include the Global Land
84 Data Assimilation System [GLDAS] (Rodell et al., 2004), “The Global Earth Observation for
85 Integrated Water Resources Assessment” [earth2Observe] (Schellekens et al., 2017), and the Global
86 Flood Awareness System [GloFAS-ERA5] (Harrigan et al., 2020). Several studies have demonstrated
87 that model-based gridded WRR products can be used as an alternative to observe river discharge in
88 poorly gauged basins to: (1) understand hydrological processes (Koukoula et al., 2020), (2) support
89 transboundary water management (Sikder et al., 2019), (3) identify flood events (Gründemann et al.,
90 2018; López et al., 2020), and (4) support national water policies (Rodríguez et al., 2020). These
91 examples demonstrate that WRR products have great potential for addressing water security
92 challenges in poorly gauged basins. Despite their numerous advantages, model outputs from WRR
93 are also fraught with uncertainties resulting from errors in the forcing data, model structure, and the
94 parameterisation of the physical processes in the model scheme (Koukoula et al., 2020). Therefore, it
95 is necessary to evaluate the performance of these products against observed river discharge where
96 available.

97 Whilst the use of outputs from WRR in water management has gained significant attention in
98 many ungauged or poorly gauged regions such as Asia and Latin America (López et al., 2020;
99 Rodríguez et al., 2020; Sikder et al., 2019), they remain largely under-utilized in Africa. For example,
100 there are only a few case studies reporting on the use of these products in the Upper Blue Nile River
101 basin (Koukoula et al., 2020; Lakew et al., 2020) and the Zambezi River basin (Gründemann et al.,
102 2018). Considering the scale of water insecurity in Africa -compounded by acute data scarcity
103 (Nkiaka et al., 2021), we feel that evaluating the performance of gridded WRR products in Africa

104 may enhance their adoption in water management in the region. On the other hand, several studies
105 evaluating the performance of gridded data in Africa have focused mostly on precipitation (Dinku et
106 al., 2018; Satgé et al., 2020) while few studies that have evaluated gridded ET products focused on
107 large basins, (Blatchford et al., 2020; Weerasinghe et al., 2020; Mcnamara et al., 2021) and mostly
108 adopting an annual timescale. This may be attributed to the large scale of the basins which is ideal
109 for the application of satellite data and the coarse spatial resolution of some of the ET products. The
110 availability of high spatial and temporal resolution ET products suggest that it now possible to
111 evaluate these products in small- to medium-size basins and at a higher temporal resolution. Lastly,
112 considering that the water balance concept has been used widely to evaluate gridded ET products,
113 most studies did not account for uncertainties in basin-wide water balance evapotranspiration (ET_{WB})
114 even though such uncertainties could be large (Baker et al., 2021).

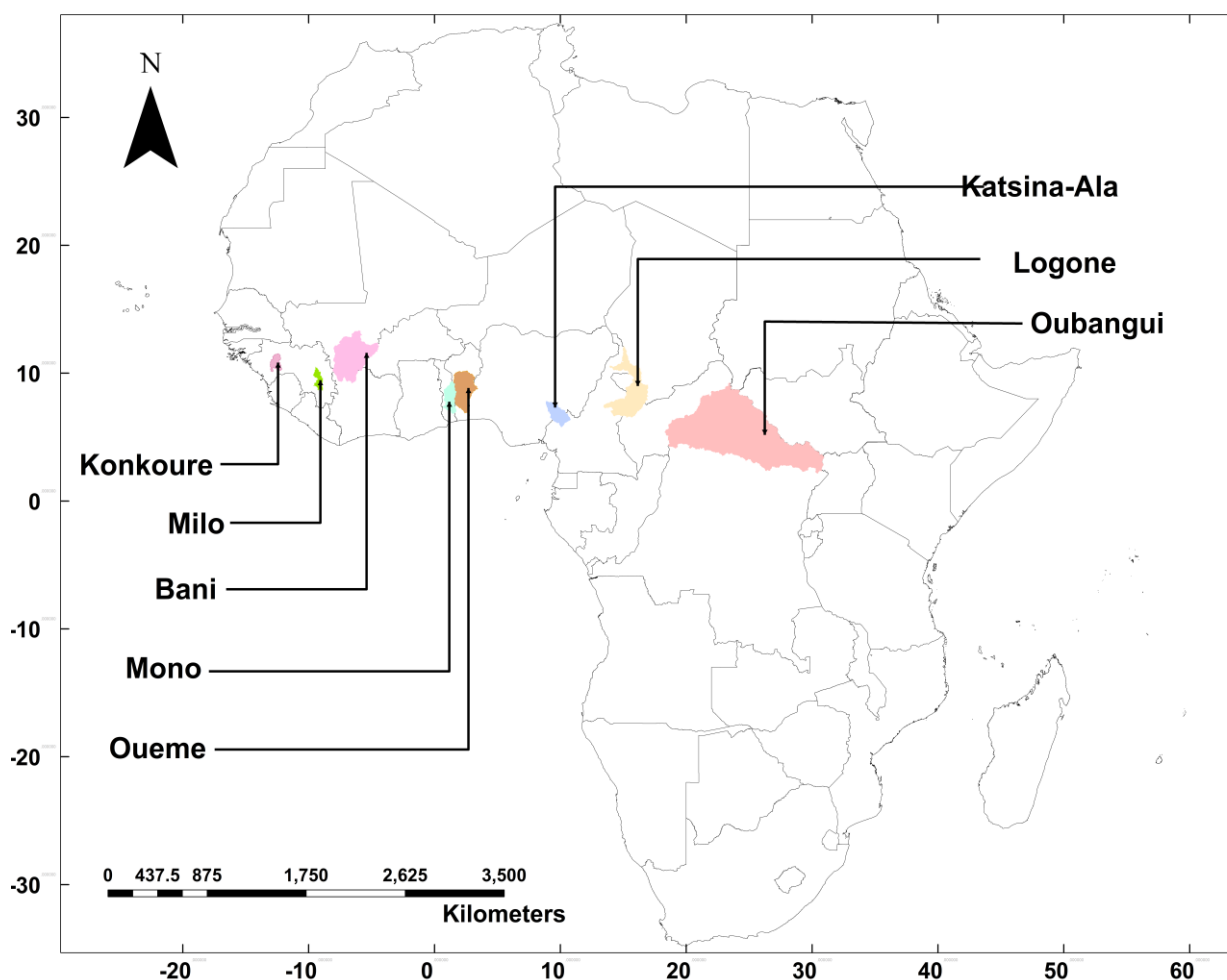
115 The objectives of this paper were to: (1) evaluate the performance of earthH2Observe Tier 1
116 and other WRR products in simulating discharge and evapotranspiration in selected small to medium-
117 size basins in Central-West Africa, (2) evaluate the performance of six satellite-based gridded ET
118 estimates and ET estimates obtained using the complimentary relationship (CR-ET) and (3) estimate
119 the relative uncertainties in ET_{WB} in the basins. Considering that only a few studies have attempted
120 to evaluate gridded WRR and ET products over Africa, this paper contributes to the contemporary
121 debate on the performance of these products and how there can be used to assess water security in
122 poorly gauged basins. We evaluated ET estimates from WRR and other sources considering that users
123 needs for the application of these products may vary. Hence our evaluation covered a wide range of
124 models and products to align with the needs of different users.

125 **2. Materials and methods**

126 **2.1. Study area**

127 The selected basins are located in Central-West Africa ranging in size from 9,000 km² to 499,000
128 km² (Figure 1). Rainfall in the region is mostly controlled by the north-south movement of the
129 intertropical convergence zone (ITCZ). The main criteria for selecting the basins were: (1) availability
130 of observed river discharge data and (2) for the period of the available discharge data to coincide with
131 the period when gridded WRR and ET data are also available. Additionally, some of the selected
132 basins currently face substantial water security challenges caused by population displacement from
133 conflicts in the Sahel and Lake Chad regions (Kamta et al., 2021; Nagabhatla et al., 2021). The
134 evaluation timestep was determined by the timestep of river discharge data. Shapefiles for all the
135 basins were obtained from HydroSHEDS, locations of the discharge gauging stations were obtained
136 from the respective data sources while the area of each basin was calculated from the basin shapefiles.
137 HydroSHEDS drainage network offers the unique opportunity to generate watershed boundaries for

138 GRDC gauging stations using a proofed dataset and applying a consistent methodology. Table 1
 139 shows that some of the basins are transboundary in nature.



140
 141 **Figure 1:** Locations of the eight river basins where the performance of WRR and gridded ET
 142 products were evaluated

143 **Table 1:** Characteristics of river basins and sources of river discharge data

Basin	Total area (km ²)	Transboundary (Yes or No) Countr(y/ies)	Population (thousands)	Source of river discharge data
Bani	101,600	(Yes) Ivory Coast, Mali, and Burkina Faso	63,766	GRDC
Katsina-Ala	22,963	(Yes) Cameroon and Nigeria	219,875	NHSA
Konkoure	10,250	(No) Guinea-Conakry	13,053	GRDC
Logone	87,953	(Yes) Cameroon, Chad, and Central Africa Republic	44,272	LCBC
Milo	9,620	(No) Guinea-Conakry	13,053	GRDC
Mono	21,575	(Yes) Togo, Benin	21,479	Co-author
Oubangui	499,000	(Yes) Central Africa Republic and the Democratic Republic of Congo	88,742	GRDC
Oueme	46,990	(No) Benin	11,488	Co-author

144 Global River Discharge Centre [GRDC], Nigeria Hydrological Services Agency [NIHSA], Lake Chad Basin Commission
 145 [LCBC]. Population data sourced from (Undesa, 2019)

146

147

148

149 **2.2. Input data**

150 **2.2.1. Water resources reanalysis (WRR)**

151 The WRR product evaluated in this study include “The Global Earth Observation for Integrated Water
 152 Resources Assessment” (earth2Observe), Famine Early Warning Systems Network [FEWS NET]
 153 Land Data Assimilation System (FLDAS), and TerraClimate. The earth2Observe Tier 1 product
 154 consists of a multi-model ensemble of ten global models at a spatial resolution of 0.5° x 0.5° spanning
 155 from 1979 to 2012 and driven by Watch Forcing Data methodology applied to ERA-Interim
 156 reanalysis (WFDEI) data (Schellekens et al., 2017). WRR data from earth2Observe are freely
 157 available at (<https://wci.earth2observe.eu/portal/>). Model evaluation here omits the Joint UK Land
 158 Environment Simulator (JULES), Simple Water Balance Model (SWBM), and the simple conceptual
 159 HBV hydrological model (HBV-SIMREG) as data from the models was not available from the portal
 160 for the selected basins at the time of writing. As such, seven models and model ensemble were
 161 included in this study. Evaluation of ET data also omits Lisflood model as data was not available
 162 from the portal at the time writing. Although there is an available Tier 2 product with a higher spatial
 163 resolution (0.25°), this study did not utilise these data as selected basins were not included at the time
 164 of conducting this research. We also evaluated discharge data from FLDAS-Noah and TerraClimate
 165 with spatial resolutions of 0.1° and 0.041° respectively. Table 2 provides a brief summary of the
 166 different models used in this study.

167 **Table 2:** Water resources reanalysis (WRR) products evaluated

Model provider	Model name	Model type	Routing scheme	Reference
CNRS (Centre National de la Recherche Scientifique)	ORCHIDEE (Organizing Carbon and Hydrology in Dynamic Ecosystems)	LSM	Cascade of linear reservoirs	(Krinner et al., 2005)
CSIRO (Commonwealth Scientific and Industrial Research Organization)	AWRA-L (Australian Water Resources Assessment)	GHM	Cascade of linear reservoirs	(Van Dijk et al., 2014)
ECMWF (European Centre for Medium-Range Weather Forecasts)	HTESEL (Hydrology Tiled ECMWF Scheme for Surface Exchanges over Land)	LSM	CaMa-Flood	(Balsamo et al., 2009)
JRC (Joint Research Centre)	LISFLOOD	GHM	Double kinematic wave	(Van Der Knijff et al., 2010)
UniUt (Universiteit Utrecht)	PCR-GLOBWB	GHM	Travel time	(Van Beek et al., 2011)
MeteoFr (Meteo France)	SURFEX	LSM	TRIP with stream	(Decharme et al., 2010)
UniK (Universitat Kassel)	WaterGAP	GHM	Manning–Strickler	(Wada et al., 2014)
NASA	Noah	LSM	Soil-layer water and energy balance	(McNally et al., 2017)
University of California Merced	TerraClimate	GHM	Bucket type model	(Abatzoglou et al., 2018)

168

2.2.2. Evapotranspiration products

169
170 In addition to the ET estimates from the reanalysis products, we also evaluated several satellite-based
171 ET estimates including GLEAM3.5a & 3.5b, MODIS16A2, PMLV1, PMLV2, SSEBop and ET
172 estimates obtained through complimentary relationship (Table 3). ET products from WRR have the
173 same spatial resolution with the discharge estimates while remote sensing products have different
174 spatial resolutions. However, we did not resample the ET data to the same resolution because a
175 previous study has shown that resampling does not have any significant impact on the results
176 (Weerasinghe et al., 2020). Table 3 provides a summary of all ET products evaluated in this study.

177 **Table 3: Summary of the characteristics of the different ET products**

ET product	Core equation	Temporal resolution	Spatial resolution	References
GLEAM3.5a & 3.5b	Priestley-Taylor	Monthly	0.25° x 0.25°	(Martens et al., 2017)
MODIS16A2	Penman-Montieth	8-day	1/48°x1/48°	(Mu et al., 2007; Mu et al., 2011)
PMLV1	Penman-Monteith-Leuning	Monthly	0.5° x 0.5°	(Zhang et al., 2016)
PMLV2	Penman-Monteith-Leuning	8-day	1/192°x1/192°	(Zhang et al., 2019)
SSEBop	Surface Energy Balance	Monthly	1/96° x 1/96°	(Senay et al., 2013)
CR-ET	Penman-Montieth	Monthly	0.25°	(Ma et al., 2021)

178

2.3. Evaluation data

179

2.3.1. River discharge

180

181 Observed river discharge data were used to evaluate the performance of WRR models and to estimate
182 basin-wide water balance evapotranspiration (ET_{WB}) using the water balance concept. The source of
183 the river discharge data is available in Table 1. Gaps in the discharge data were filled using Self-
184 Organizing Maps which which is a robust method for infilling missing gaps in hydrometeorological
185 time series (Nkiaka et al., 2016).

2.3.2. Precipitation

186

187 Climate Hazards Group InfraRed Precipitation with Station data (CHIRPS) was used to estimate
188 ET_{WB} . CHIRPS has a quasi-global coverage at a spatial resolution of 0.05° x 0.05°, spanning the
189 period from 1981 to the present at a daily timescale (Funk et al., 2015). The dataset was designed
190 taking into consideration the weaknesses of existing products (Sulugodu et al., 2019). As such,
191 CHIRPS blends gauge and satellite precipitation covering most global land regions, it has low latency,
192 high resolution, low bias, and long period of record (Funk et al., 2015). CHIRPS has extensively been
193 validated (Dinku et al., 2018; Satgé et al., 2020) and used in several studies in Africa (Larbi et al.,
194 2021; Nkiaka, 2022). The data was downloaded as the spatial average for each basin using the Climate
195 Engine App.

196
197
198
199
200
201
202
203
204
205
206
207
208
209
210
211
212
213
214
215
216
217
218
219
220
221
222
223
224
225
226
227

2.3.3. GRACE

GRACE data are monthly anomalies of terrestrial water storage changes (TWSC) used to quantify changes in terrestrial water storage. The dataset has a global coverage spanning the period 2003–2017 (Tapley et al., 2019). The data was derived from Jet Propulsion Laboratory (JPL) RL06M Version 2.0 GRACE mascon solution at a spatial resolution of $0.5^\circ \times 0.5^\circ$. The data has a coastline resolution improvement (CRI) filter to reduce leakage errors across coastlines and land-grids, using scaling factors derived from the community land model (Wiese et al., 2016). GRACE data has recently been re-processed to reduce measurement errors and represents a new generation of gravity solutions that do not require empirical post-processing to remove correlated errors, as such, the present data is better than the previous GRACE version that was based on spherical harmonic gravity solution (Wiese et al., 2016). GRACE data was used in this study to estimate ET_{WB} following the approach used in several studies e.g., (Andam-Akorful et al., 2015; Liu, 2018; Xie et al., 2022).

2.4. Evaluating gridded WRR

WRR models were evaluated following a multi-objective approach commonly used in evaluating the performance of hydrological models, including the Nash-Sutcliffe efficiency (NSE), Kling-Gupta efficiency (KGE), and the percent bias (PBIAS). NSE scores range from $-\infty$ to 1, with 1 indicating a perfect representation of observed discharge. NSE scores ≥ 0.50 can be considered acceptable whereas NSE scores ≤ 0.0 indicate poor model performance (Moriasi et al., 2007). Similarly, the KGE is a dimensionless metric that can be decomposed into three components crucial for evaluating hydrological model performance accounting for temporal dynamics (correlation), bias errors (observed vs simulated volumes), and variability errors (relative dispersion between observations and simulations) (Gupta et al., 2009). KGE scores range from $-\infty$ to 1, with 1 considered the ideal value. Next, PBIAS is used to measure the tendency of the simulated discharge to be larger or smaller than their observed counterparts (Gupta et al., 2009). PBIAS is expected to be 0.0, with low magnitude values indicating accurate simulations, positive values indicate underestimation, negative values indicate overestimation (Moriasi et al., 2007). According to Moriasi et al. (2007), a hydrological model with PBIAS values in the range $\pm 25\%$ can be considered to be acceptable. Furthermore, a temporal evaluation of flow hydrographs was carried out by plotting the monthly simulated vs observed discharge to ascertain visually if the models were able to capture the magnitude, seasonality, and interannual variability of discharge.

Table 4: Contingency table for 80th percentile river discharge

	Observed discharge	
	Yes	No
Simulated discharge	Yes	Hits (H) False Alarms (FA)
	No	Misses (M) Correct Negatives

228 Lastly, we evaluated the models ability to predict discharge above specific thresholds. This evaluation
 229 step is of critical importance when considering operational water management requirements such as
 230 water allocation and reservoir operation which rely on monthly river discharge. To achieve this, we
 231 adopted the Critical Success Index (CSI) as the metric to evaluate the ability of each model to simulate
 232 discharge at 20th and 80th percentiles (i.e. discharge at 80th and 20th percent exceedance respectively).
 233 CSI is calculated from a two-dimensional contingency table defining the events in which observed
 234 and simulated discharges exceed a given threshold (Thiemig et al., 2015). We used the 20th and 80th
 235 percentiles to assess the ability of the models to simulate both low and high flows respectively. The
 236 contingency table (Table 4) is a performance measure used in summarizing all possible forecast-
 237 observation combinations such as hits (H; event forecasted and observed), misses (M; event observed
 238 but not forecasted), false alarms (FA; event forecasted but not observed) and correct negatives (CN;
 239 event neither forecasted nor observed). The ideal value for CSI is 100% and the metric is calculated
 240 as follows:

$$241 \quad CSI = \frac{H}{H + M + FA} \times 100 \quad (1)$$

242 **2.5. Evaluating gridded ET**

243 We also adopted a multi-step approach to evaluate the performance of ET products by assessing the
 244 annual ET–precipitation ratio, evaluating the statistical performance of ET products against long-term
 245 ET_{WB} and the ability of the products to capture monthly ET variability.

246 In the first step, the annual ET–precipitation ratio was calculated to compare with the ratio
 247 obtained using ET_{WB} method. The ET–precipitation ratio can also provide an estimate of the amount
 248 of water available in each basin after evapotranspiration losses. In the second step, different statistical
 249 metrics were used to assess the performance of the ET products using the monthly ET_{WB} as a reference
 250 (Andam-Akorful et al., 2015; Burnett et al., 2020; Koukoulou et al., 2020). The monthly ET_{BW} was
 251 calculated using the basin water balance equation as follows:

$$252 \quad ET_{WB} = P - Q - \Delta S \quad (2)$$

253 Where P is average monthly precipitation over the basin (mm), Q is river discharge (mm) and ΔS is
 254 the terrestrial water storage change [TWSC] (mm). Unlike several studies that have evaluated ET
 255 products on an annual timescale, this study adopts a monthly sample. As such, the TWSC component
 256 (ΔS) in equation 2 that is often neglected when estimating ET_{WB} over several years (≥ 10 years) could
 257 not be overlooked. Due to the likely impact of anthropogenic activities such as reservoir operation,
 258 water withdrawal, and monthly rainfall variability on TWSC, values derived at monthly timescales
 259 are important. TWSC data used in this study were obtained from GRACE.

260 Due to the coarse spatial resolution of GRACE, it has been argued that GRACE is not sensitive
 261 at detecting changes in monthly TWSC in small-size basins $\leq 150,000 \text{ km}^2$ (Rodell et al., 2011). Based
 262 on this claim, it might be argued that GRACE data may not be applicable in this study considering
 263 that most of the basins are below this threshold except the Oubangui ($499,000 \text{ km}^2$). However, several
 264 studies (Liu, 2018; Biancamaria et al., 2019; Oussou et al., 2022; Xie et al., 2022), have demonstrated
 265 that GRACE can provide acceptable TWSC estimates for basins that are smaller than this threshold.
 266 Encouraging results from these and other studies do therefore suggest that GRACE data can be used
 267 in this study; albeit with the expectation of considerable uncertainties in TWSC estimates. For this
 268 study, GRACE data for each basin were obtained by averaging the timeseries of all coincident
 269 GRACE grid cells. To estimate changes in monthly TWSC, we calculated the difference between
 270 consecutive GRACE measurements for each basin, divided by the time between measurements, using
 271 the following equation:

$$272 \quad \Delta S = (S_{[n]} - S_{[n-1]})/dt \quad (3)$$

273 Where ΔS represents the TWSC (mm), n is the measurement number, and dt is the time difference
 274 between two consecutive GRACE measurements (months).

275 Lastly, temporal evaluation of the products was carried out by plotting the time series of all
 276 ET products against ET_{WB} to visually establish if the gridded ET products were able to capture the
 277 magnitude, seasonality, and interannual variability of ET across the basins.

278 **2.6. Estimating relative uncertainty in basin-scale water balance ET (ET_{WB})**

279 To estimate the relative uncertainty in monthly ET_{WB} , we first calculated the absolute uncertainty in
 280 monthly ET_{WB} by propagating errors through each of the components in equation 2 (Rodell et al.,
 281 2011), as follows:

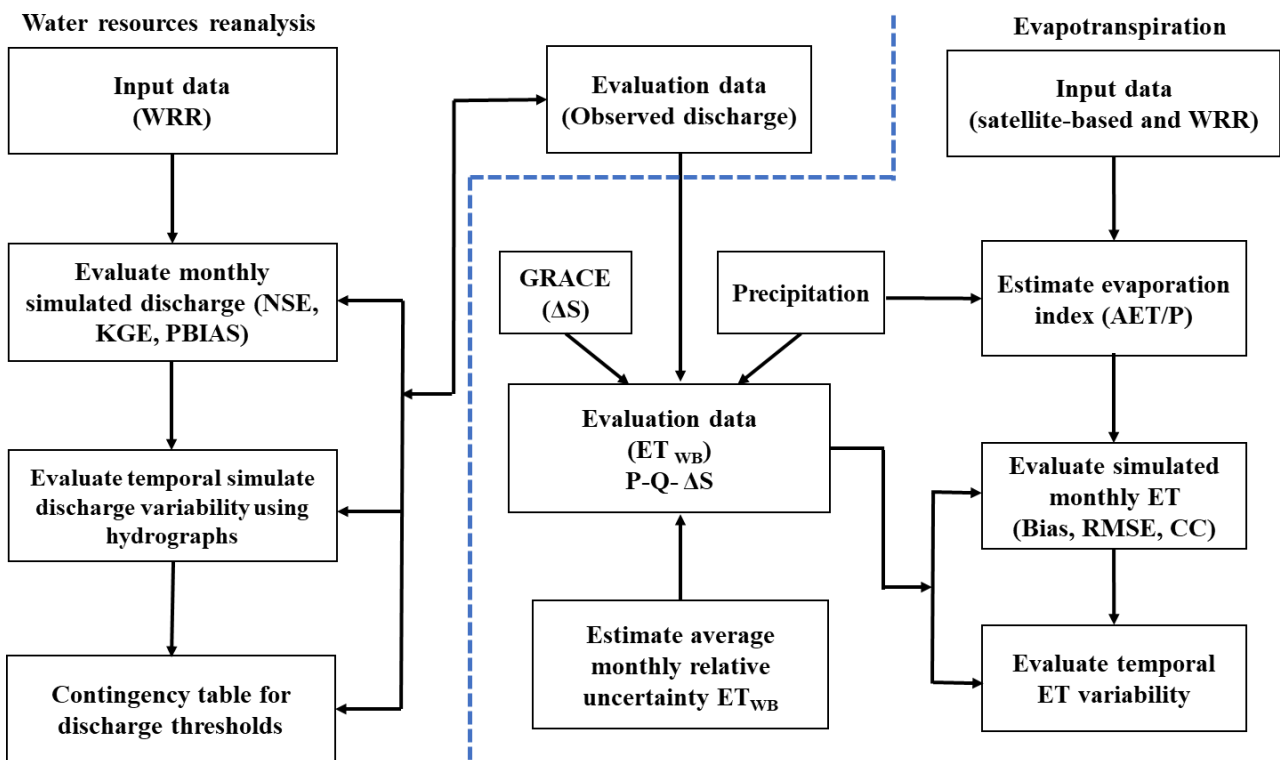
$$282 \quad \sigma_{ET} = \sqrt{\sigma_P^2 + \sigma_Q^2 + \sigma_{\Delta S}^2} \quad (4)$$

283 Where σ_P , σ_Q and $\sigma_{\Delta S}$ represent the absolute uncertainties in basin precipitation, observed river
 284 discharge, and TWSC respectively. Uncertainty in precipitation was estimated as systematic errors
 285 (bias). For this, we used a value of 2 % estimated for CHIRPS data at monthly timescale from 1981–
 286 2016 over Africa from a validation study using the Global Precipitation Climatology Centre (Shen et
 287 al., 2020). Uncertainty in TWSC was determined using the gridded fields of measurement and leakage
 288 errors (residual errors after filtering and rescaling) that are provided with the GRACE data. The
 289 uncertainty for each basin was calculated by averaging the values of all GRACE grid cells within
 290 each basin. To account for month-to-month variation in equation 3, the TWSC error values were

291 multiplied by $\sqrt{2}$ to obtain $\sigma_{\Delta S}$ (Andam-Akorful et al., 2015). Because no uncertainty estimates were
 292 provided with the river discharge data, we adopted a value of 20 % which has been used in a recent
 293 study in the region (Burnett et al., 2020). After estimating the absolute uncertainty in monthly ET_{WB} ,
 294 the relative monthly uncertainty was calculated using equation 5 (Baker et al., 2021) as follows:

$$295 \quad vET = \frac{\sigma ET}{ET_{WB}} \times 100 \quad (5)$$

296 Where vET is the monthly relative uncertainty (%), σET is the absolute monthly uncertainty (mm),
 297 and monthly ET_{WB} (mm). Figure 2 shows a flowchart detailing the different steps used for evaluating
 298 the WRR and ET products.



299
 300 **Figure 2:** Flowchart outlining the steps used in evaluating the WRR and ET products (The blue
 301 dotted line in the flow chart separates evaluation of WRR from ET products)

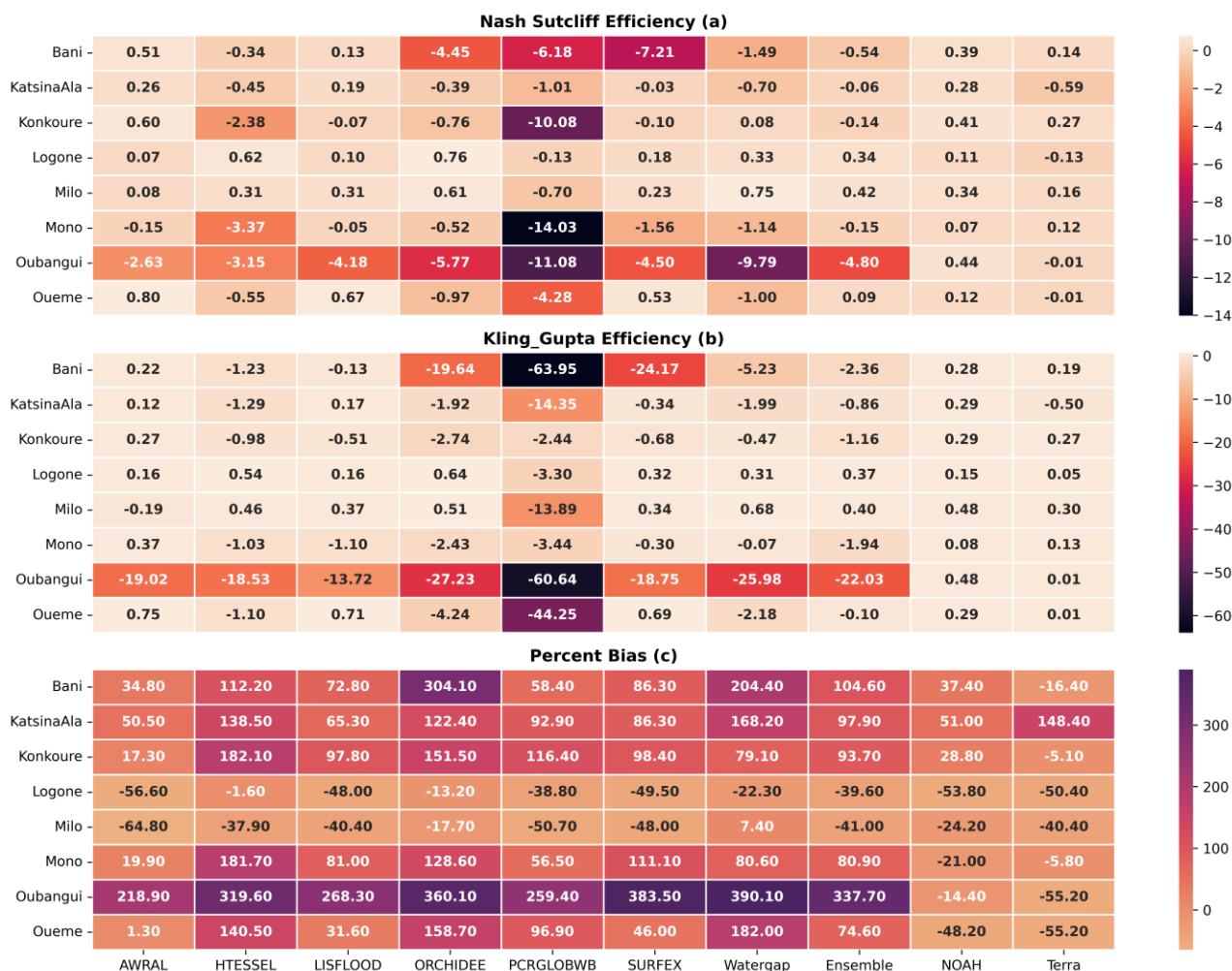
302 3. Results

303 3.1. Water resources reanalysis products

304 3.1.1. Hydrological performance

305 A multi-objective approach using different statistical metrics (NSE, KGE and PBIAS) was used to
 306 evaluate discharge estimates from WRR products. The performance of the models in simulating
 307 discharge is shown in Figure 3. Using the NSE as a performance metric, results show that Noah
 308 produced positive scores in all the basins (0.15–0.48). Terra, AWRAL and Lisflood produced positive
 309 scores (0.01–0.75) in seven, six and four basins respectively. SURFEX model produced positive

310 scores in three basins while ORCHIDEE, HTESSSEL, Watergap and the ensemble mean produced
 311 positive scores in two basins each while PCR-GLOBW produced negative scores in all the basins
 312 (Figure 3a).



313
 314 **Figure 3:** Statistical evaluation of the models using (a) NSE, (b) KGE, and (c) PBIAS. Red and
 315 orange colours represent poor model performance in Figures 3a, 3b & 3c, however, the acceptable
 316 PBIAS range in Figure 3c is $\pm 25\%$. Ensemble refers to the mean of WRR from the earthH2Observe.

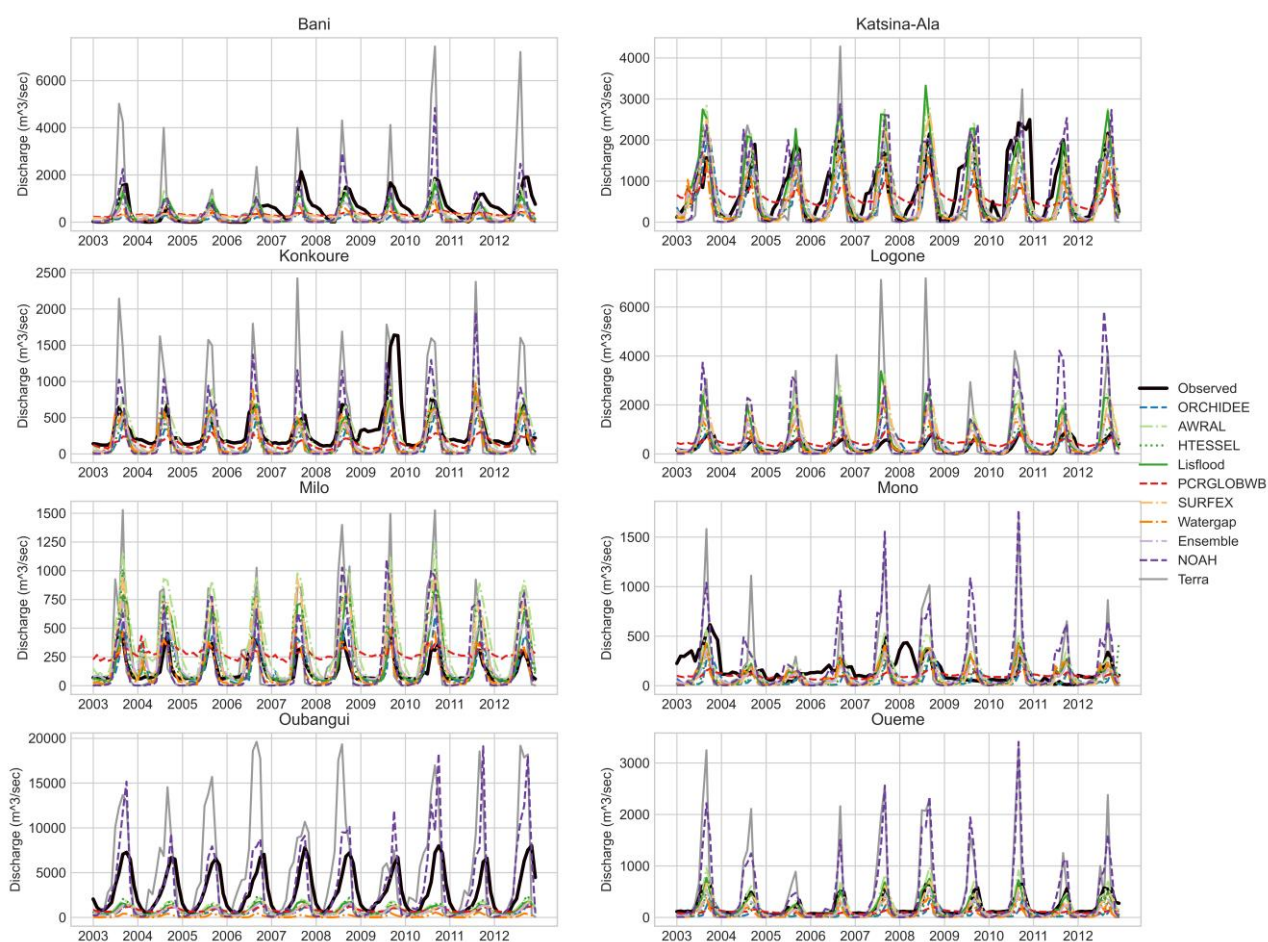
317 KGE results show that Noah also produced positive scores (0.11– 0.44) in all basins, followed by
 318 AWRAL, Lisflood and Terra with positive scores in six, five and four basins respectively (Figure
 319 3b). SURFEX and Watergap produced positive scores in three basins while ORCHIDEE and
 320 HTESSSEL produced positive scores (0.31–0.76) in two basins. The ensemble mean produced positive
 321 scores (0.09 – 0.42) in three basins while PCRGLOBW produced the lowest KGE scores (Figure 3b).

322 Positive and negative PBIAS values were obtained in the different basins. Negative values
 323 indicate that the model overestimated discharge volumes compared to observed discharge while
 324 positive values indicate the opposite. Noah, Terra and AWRAL produced acceptable PBIAS scores
 325 ($\pm 25\%$) in three basins, ORCHIDEE and Watergap produced similar scores in two basins and

326 HTESSEL in one basin (Figure 3c). The rest of the models including the ensemble mean either grossly
 327 overestimated or underestimated discharge volumes in all the basins.

328 3.1.2. Temporal evaluation

329 The ability of the models to capture discharge variability was analysed by comparing the simulated
 330 vs observed discharge. Results show that most of the models were able to capture the seasonal
 331 discharge variability including peak and low flows (Figure 4). However, PCR-GLOBW
 332 systematically overestimated low flows and underestimated high flows across all basins. In the
 333 Oubangui basin, all models were able to capture the seasonal variability but consistently
 334 underestimated peak flows except Noah and Terra models which both overestimated peak flows
 335 (Figure 4). For example, measured peak discharge in the river exceeds 5000 m³/sec, but all models
 336 except Noah and Terra simulated it to be less than 2000 m³/sec (Figure 4).

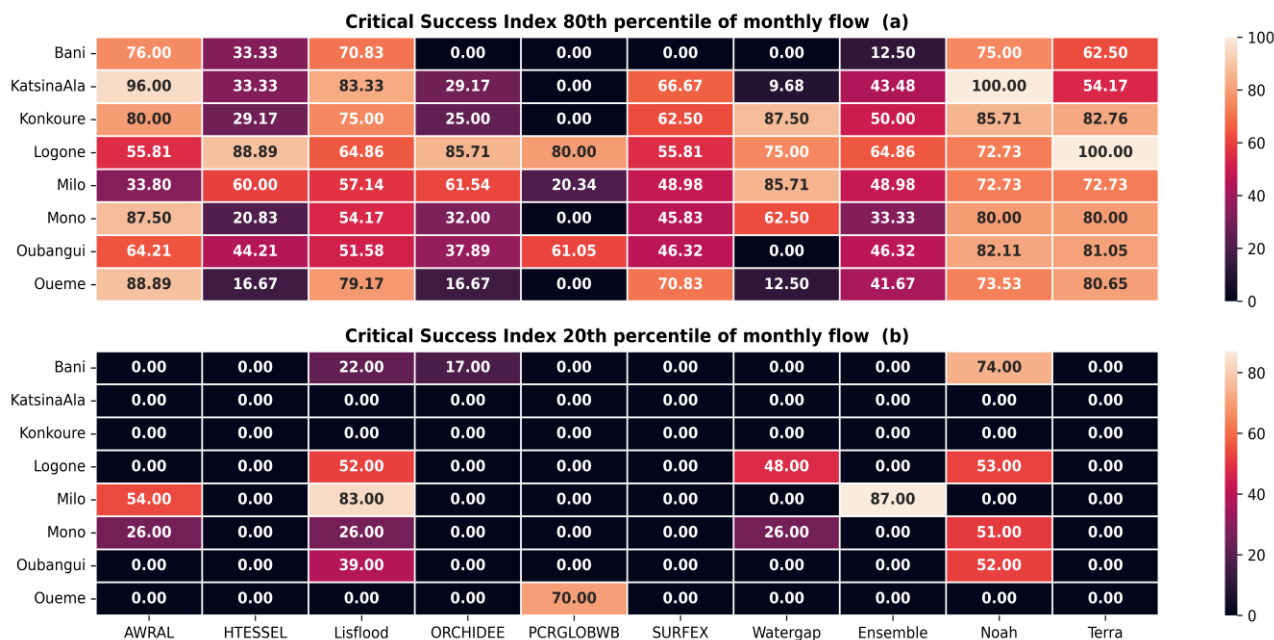


337
 338 **Figure 4:** Evaluation of temporal flow variability simulated by the different model

339 3.1.3. Critical Success Index

340 Figure 5 shows the performance of the models in simulating the 80th and 20th percentiles monthly
 341 discharge. For the 80th percentile flows, results show that Noah and Terra produced CSI scores above
 342 50 % in all basins followed by Lisflood and AWRAL in seven and six basins respectively while
 343 Surfex and Watergap produced similar scores in four basins each (Figure 5a). For the 20th percentile

344 flows, only Noah produced CSI scores above 50 % in four basins while Lisflood produced similar
 345 scores in two basins. The performance of the other models in simulating the 80th percentile flow
 346 shows a large spread while most models including the ensemble mean failed to simulate the 20th
 347 percentile flow across all the basins. Taking together, results suggest that the models simulated high
 348 flows better than the low flows with only Noah capable of capturing both flow regimes in most basins
 349 (Figure 5b).

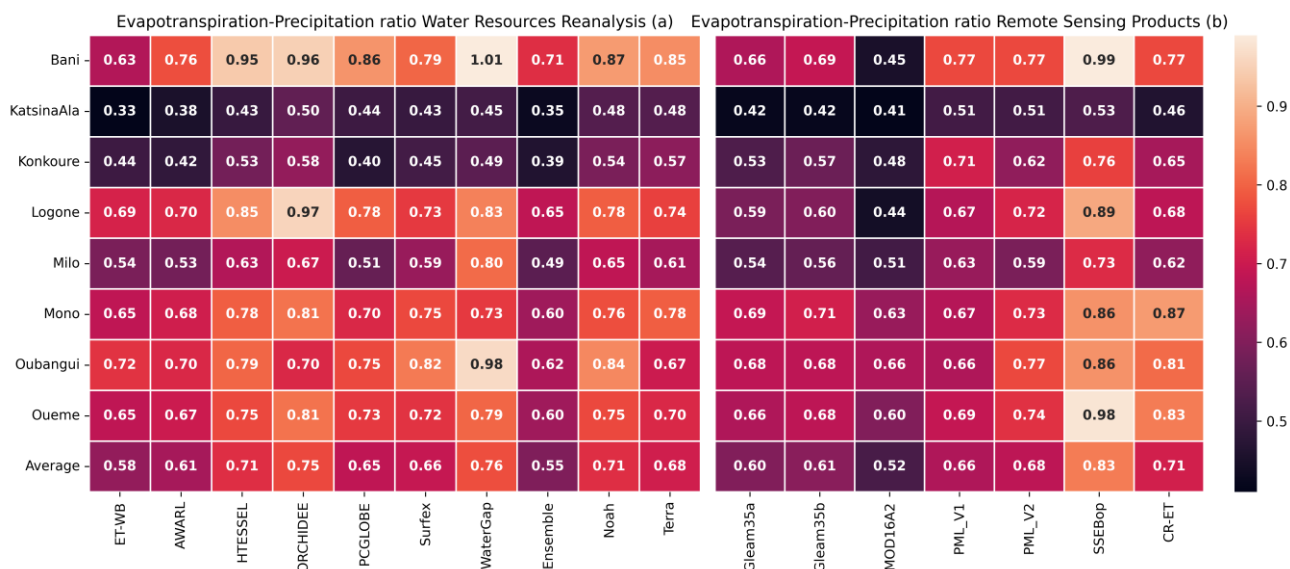


350
 351 **Figure 5:** Critical Success Index for 80th and 20th percentile of monthly flow across all basins

352 **3.2. Evapotranspiration products**

353 **3.2.1. Evapotranspiration–precipitation ratio**

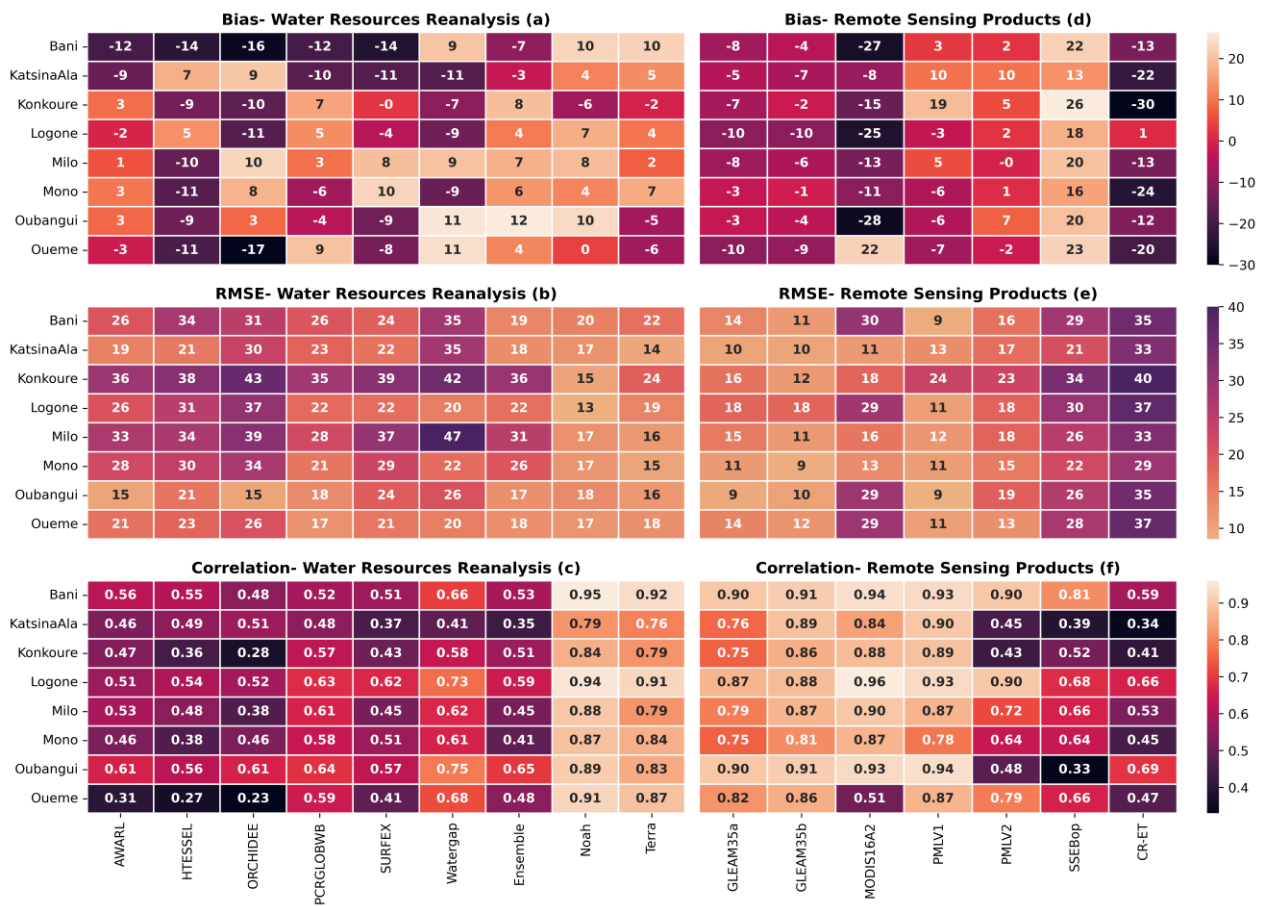
354 Figure 6 shows the annual ET–precipitation ratio for all basins. It can be observed that average annual
 355 ET–precipitation ratio ranges between (0.58–0.76) for WRR and (0.52–0.83) for satellite-based
 356 products over a period of 10 years (2003–2012) across all basins. WaterGap produced the highest
 357 ratio (0.45-1.01) among WRR models, SSEBop produced the highest ratio (0.53–0.99) while
 358 MOD16A2 produced the lowest ratio (0.41–0.66) among the satellite-based products (Figure 6).
 359 Results show that the evaporation ratios from the different ET estimates are in the same order of
 360 magnitude with the ratio from ET_{WB} across all the basins except for WaterGap, SSEBop, MOD16A2
 361 and CR-ET which produced values which were beyond this range (Figure 6).



362
363 **Figure 6:** Annual evapotranspiration – precipitation ratio 2003 – 2012

364 **3.2.2. Basin-wide water balance estimates**

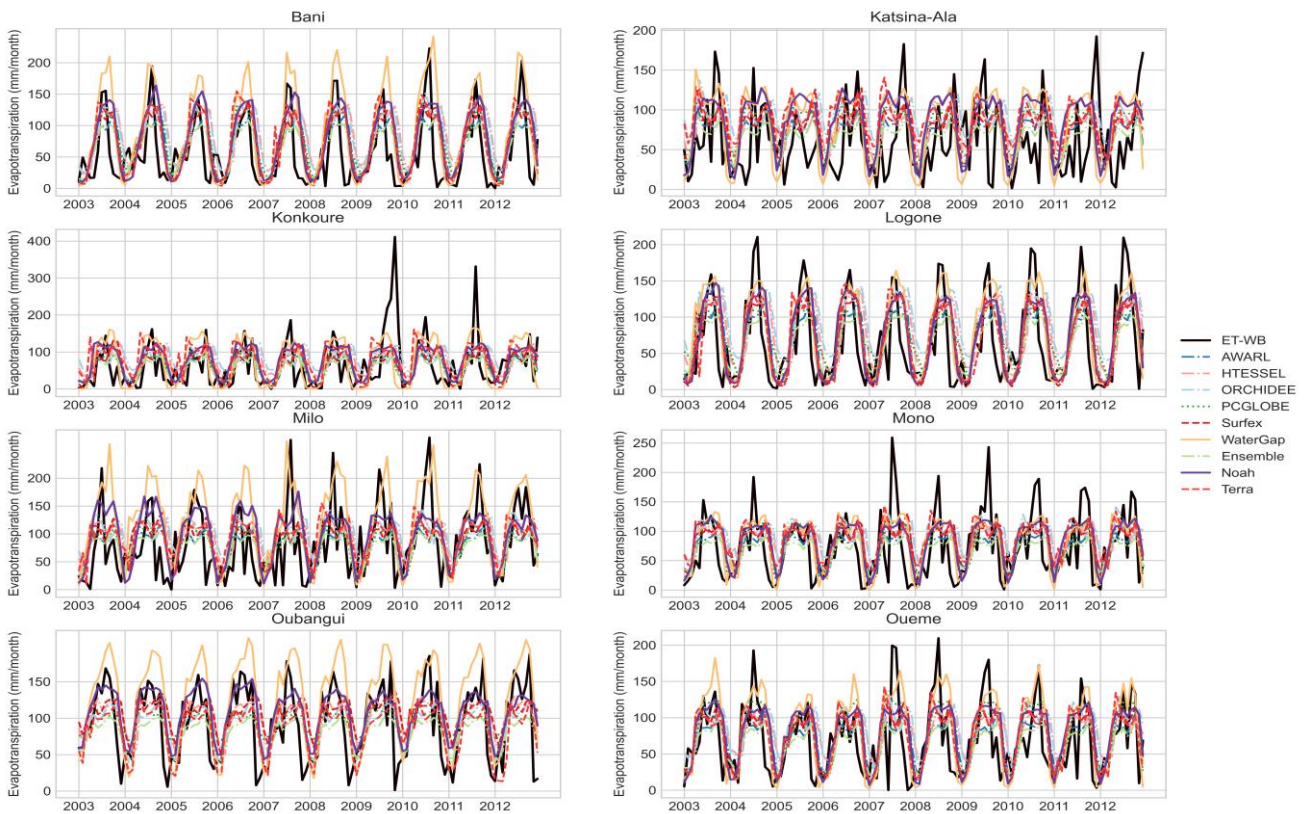
365 Figure 7 shows the results of the statistical metrics used in evaluating the ET estimates using monthly
 366 ET_{WB} as reference. Considering bias as a performance metric, AWARL, Noah and Terra produced
 367 the lowest bias scores among WRR products while PMLV2, Terra, and GLEAM3.5a & 3.5b produced
 368 the lowest bias scores among the satellite-based products (Figure 7a&d). Most WRR products
 369 underestimated ET and similarly GLEAM also slightly underestimated ET, among the satellite-
 370 based products while the rest of the products produced mixed results (Figure 7a&d). However,
 371 SSEBop systematically overestimated ET in all the basins while MOD16A2 grossly underestimated
 372 this variable in all but one basin with respect to monthly ET_{WB} (Figure 7d).



373

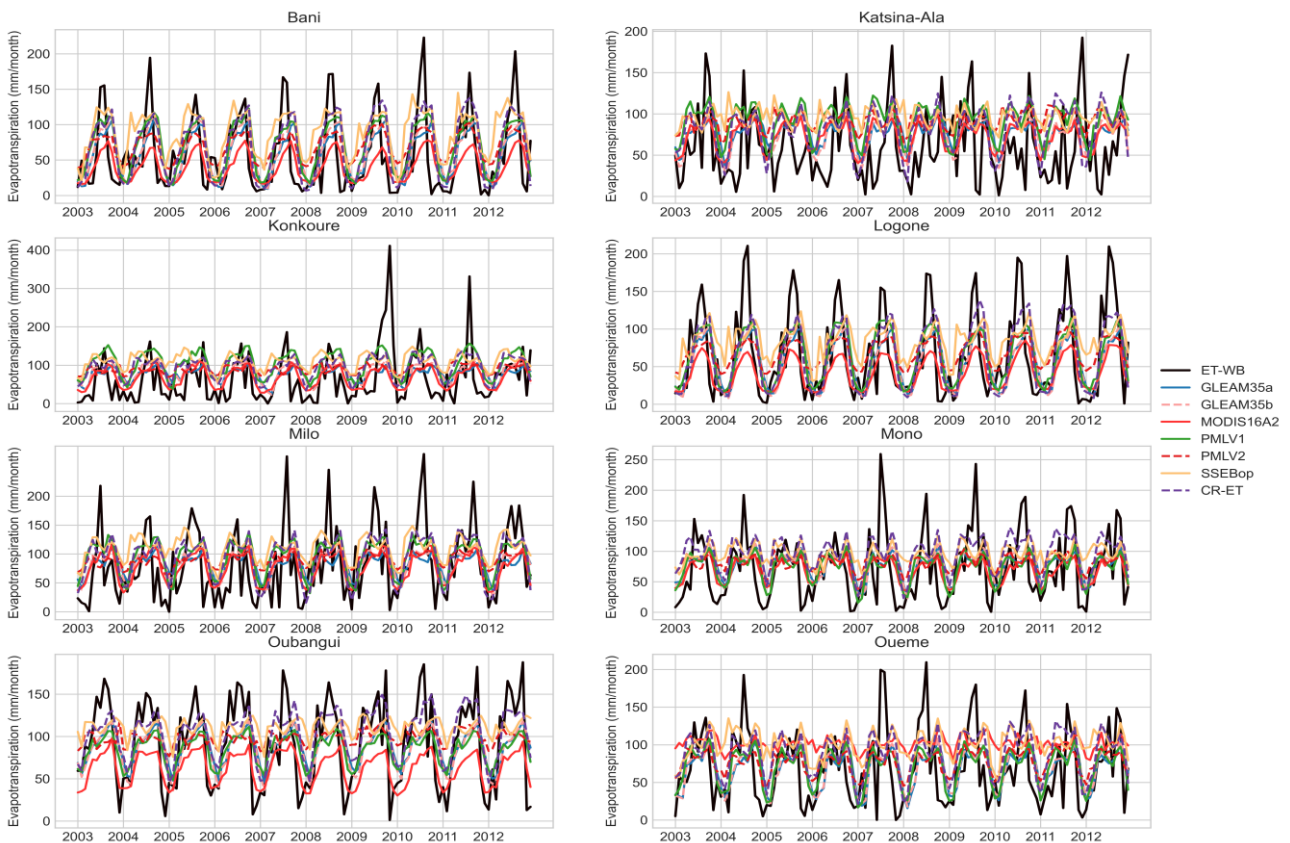
374 **Figure 7:** Bias, RMSE, and Pearson correlation coefficient between monthly ET_{WB} and different
 375 ET products (a-c: WRR and d-f: remote sensing products).

376 Noah produced the lowest RMSE (13–20 mm/month) among the WRR products while GLEAM3.5a
 377 & b and PMLV1 produced the lowest RMSE (8.50–12 mm/month) among the satellite-based products
 378 (Figure 7b&e). The rest of the products both WRR and satellite-based produced substantially higher
 379 RMSE scores (Figure 7b&e). Among WRR products, only Noah and Terra produced high Pearson
 380 correlation scores across all basins (Figure 7c). On the other hand most satellite-based products
 381 produced high Pearson correlation scores (≥ 0.75) in all basins except PMLV2 and SSEBop which
 382 both produced low scores (< 0.50) in three and two basins respectively (Figure 7f). ET estimates
 383 produced from complimentary relationship (CR-ET) performed poorly across most basins.



384

385 **Figure 8a:** Seasonal cycle of ET estimates from WRR and basin-wide water balance
 386 evapotranspiration. ET_{WB} represents monthly evapotranspiration estimated by the water balance
 387 method, while the rest are derived from LSMs and GHMs.



388

389 **Figure 8b:** Seasonal cycle of ET estimates from remote sensing-based products and basin-wide water
 390 balance evapotranspiration.

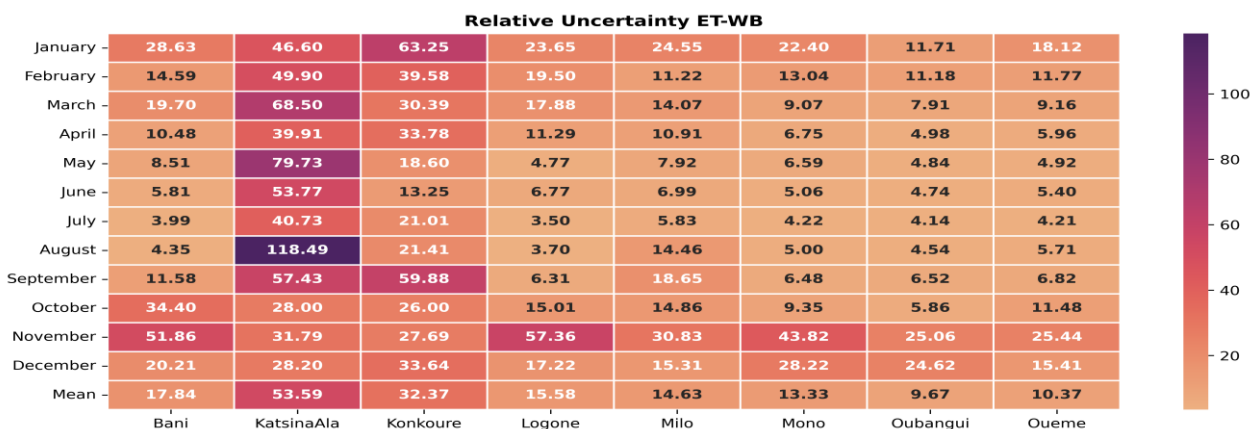
391 **3.2.3. Monthly ET variability**

392 Figure 8 shows the seasonal cycle of ET_{WB} against both WRR products and satellite-based ET
 393 estimates. It can be observed that most products were able to replicate the seasonal ET cycle across
 394 all the basins (Figure 8a&b). However, most products were not able to replicate the high ET peaks
 395 produced by ET_{WB} during the rainy season except WaterGap in some instances (Figure 8a). The
 396 performance of CR-ET follows that of the rest of the products.

397 **3.2.4. Estimating relative uncertainty in ET_{WB}**

398 An assessment of absolute uncertainties in monthly ET_{WB} indicated that the dominant sources of
 399 uncertainty vary from one basin to another and by each month. For example, in the Katsina-Ala,
 400 Konkoure, and Milo basins, the dominant source of uncertainty in monthly ET_{WB} was river discharge
 401 (**supplementary material**). Although the absolute uncertainty in precipitation and TWS also appear
 402 to be high in the three basins, the uncertainty in river discharge takes precedence over the other
 403 sources of uncertainty due to its higher magnitude (**supplementary material**). On the contrary, the
 404 dominant source of uncertainty in ET_{WB} in the Bani, Logone, and Oubangui basins was from TWSC.
 405 Across all the basins, there was no significant variation in monthly TWSC uncertainty which is
 406 consistent with the results of a similar study in the Amazon basin (Baker et al., 2021). Results also
 407 revealed that the magnitude of TWSC uncertainty were similar across the basins irrespective of the
 408 basin size (**Supplementary material**).

409 Figure 9 shows the relative uncertainty in ET_{WB} across all the basins. It can be observed that
 410 relative uncertainty values are mostly <30 % but vary from month to month. However, the values
 411 were exceptionally high in the Katsina-Ala and Konkoure basins. The relative uncertainty in ET_{WB}
 412 also appears to be exceptionally high in the months of September–November which corresponds to
 413 the high flow season across the basins. Taking together, the average monthly relative uncertainty in
 414 ET_{WB} for all basins ranges from 10–18% except in the Katsina-Ala and Konkoure basins where this
 415 range is grossly exceeded.



416 **Figure 9:** Average (2003 – 2012) monthly relative uncertainty in monthly ET_{WB} (%)
 417

418 **4. Discussion**

419 The overarching goal of this paper was to assess the performance of gridded WRR and ET products
420 and to estimate the relative uncertainty in monthly basin-wide evapotranspiration (ET_{WB}) estimates.
421 Below we provide a discussion and implications of our results in water security assessment in poorly
422 gauged basins.

423 **4.1. Water resources reanalysis**

424 The performance of WRR products was assessed through commonly used model evaluation metrics,
425 discharge variability, and verification skill scores (critical success index) using observed river
426 discharge data. Our results show strong differences in the performance of the different models in
427 simulating river discharge across the basins. Noah model produced positive NSE and KGE values in
428 all basins and PBIAS values within the acceptable range ($\pm 25\%$) in three basins. Temporal evaluation
429 of the WRR products showed that Noah, Terra, AWRAL and Lisflood were able to capture the
430 seasonal variability in discharge as demonstrated by high KGE scores. Indeed, high KGE values
431 suggest that some models were able to capture the temporal dynamics (strong correlation), and low
432 bias scores indicate that the variability errors between the observed discharge and simulation was also
433 low (Gupta et al., 2009). Nevertheless, Terra consistently overestimated peak flows in all the basins.

434 Apart from Noah model which is a LSM used in FLDAS, most GHMs used in
435 earthH2Observe tier 1 product performed better than the LSMs, which is consistent with results from
436 other studies (Lakew et al., 2020). The strong performance of GHMs compared to LSMs can be
437 attributed to the differences in the model structure and parametrisation schemes between LSMs and
438 GHMs (Gründemann et al., 2018; Koukoula et al., 2020). For example, some GHMs such as
439 Watergap are able to simulate lakes and reservoirs and water withdrawal while LSMs can only
440 simulate natural processes. Such differences in model structure can significantly influence discharge
441 volumes simulated by both types of models (Gründemann et al., 2018). Although PCRGLOBW is a
442 GHM, it produced substantially low performance compared to the LSMs which is consistent with
443 results from other studies in the region (Gründemann et al., 2018; Lakew et al., 2020). This suggest
444 that PCRGLOBW model may not be suitable for assessing water security in the region.

445 The ability of the models to simulate flow thresholds was evaluated using the CSI. Results
446 show that Noah, Terra, AWRAL and Lisflood were able to capture more than 50% of 80th percentile
447 monthly flow in most basins. We also noted that apart from Noah model, the rest of the GHMs
448 performed better than the LSMs from earthH2Observe in their ability to capture the 80th percentile
449 monthly flows across the basins while only Noah was able to capture 20th percentile flows in three
450 basins. The performance of Noah compared to other models can be attributed to the fact that FLDAS
451 was specially designed and optimized to produce physically meaningful variables for monitoring food

452 and water security in data-scarce regions in Africa (McNally et al., 2017). Furthermore, Noah and
453 Terra with spatial resolutions of 0.1° & 0.041° respectively perform better than other models which
454 may be attributed to their higher spatial resolutions compared to other models with a coarser
455 resolution (0.5°). In fact, Gründemann et al. (2018), has shown that WRR products with higher spatial
456 resolution perform better than products with coarser resolution in their ability to simulate discharge.
457 The performance of Noah can also be attributed to the fact the FLDAS is driven by a combination of
458 different precipitation products thereby reducing the uncertainty in the input data while earth2observe
459 tier 1 product are driven by one data source (WFDEI) which increases the uncertainty in the input
460 data which is propagated to the model outputs. Our results also showed that Lisflood performed better
461 than most of the other earth2observe models which may be attributed to the fact that Lisflood has been
462 extensively used in research and operational settings in Africa (Thiemig et al., 2015; Smith et al.,
463 2020). As such, the model parameters may have been better constrained in the region than other
464 models from earth2Observe. Taking together, results from this study highlight the importance of
465 evaluating outputs from WRR products in representative basins before applying them in studies that
466 may have wider policy and financial implications in poorly gauged basins. Our results suggest a need
467 to enhance the spatial resolution of WRR products and for the products to be driven by input data
468 from multiple sources to reduce the uncertainties in the input data.

469 **4.2. Evapotranspiration products**

470 The annual ET–precipitation ratio produced by WRR and satellite-based ET products are within the
471 range estimated for the global land regions (Rodell et al., 2015) with the only exception being
472 WaterGap, SSEBop, MOD16A2 and CR-ET with values beyond this range. This suggests that ET
473 estimates from both sources performed well in this aspect of the ET evaluation. The annual ET–
474 precipitation ratios obtained in this study suggests that annual ET does not exceed annual precipitation
475 in most basins during the period under evaluation. This suggest the availability of sufficient water
476 resources in each basin.

477 Considering all the ET evaluation criteria and comparing between estimates from WRR and
478 satellite-based products, Noah, Terra, GLEAM3.5a & 3.5b, and PMLV2 appear to outperform the
479 rest of products even though GLEAM products slightly underestimated ET in all the basins.
480 Conversely, WaterGap, SSEBop and MOD16A2 performed poorly and may not be suitable for water
481 security assessment in the region. Our results are generally consistent with those from other studies
482 indicating that GLEAM and MODIS16A2 underestimate evapotranspiration, while SSEBop
483 overestimates this variable in most parts of Africa (Weerasinghe et al., 2020; Adeyeri and Ishola,
484 2021; Mcnamara et al., 2021). Given that ET estimates from Noah and Terra are produced together
485 with other water balance components (runoff, soil moisture and baseflow) the two models may be

486 recommended for water security assessment in the region because of water balance closure. Our
487 results also revealed that the performance of satellite-based ET products is not influence by spatial
488 resolution which is consistent with results from previous studies (Weerasinghe et al., 2020; Jiang and
489 Liu, 2021). For example, Gleam products with a spatial resolution of 0.25° outperformed products
490 such as MODIS16A2 and SSEBop with higher spatial resolutions. Conversely, ET estimates from
491 WRR appear to be influenced by spatial resolution considering that Noah and Terra with higher
492 spatial resolutions outperformed other products with coarser resolutions.

493 Although all the products were able to capture the temporal dynamics of ET in all the basins,
494 there were substantial differences in the magnitude of monthly ET from each model. This finding is
495 consistent with results from other studies showing strong differences in ET estimates produced by
496 different models (Weerasinghe et al., 2020; Adeyeri and Ishola, 2021). The discrepancies in monthly
497 ET estimates from the models may be attributed to differences in model structure, parameters, and
498 uncertainties in the input data used in driving the models. This is also in-line with findings from
499 another study in West Africa highlighting the impact of model parameters and input data uncertainty
500 on ET estimates (Jung et al., 2019). Considering the aforementioned factors, it may be difficult to
501 expect the products to produce similar results. ET_{WB} estimates across all the basins produced high
502 peaks during the rainy season which is also similar to the results of a related study in West Africa
503 (Andam-Akorful et al., 2015). The high peaks observed in ET_{WB} may be attributed to errors inherent
504 in monthly precipitation, river discharge, and TWSC estimates used in estimating monthly ET_{WB} .

505 Given that there was no uncertainty information on the river discharge data used in this study,
506 we adopted a value of 20 % following a previous study in the region (Burnett et al., 2020). In fact,
507 we feel that this value may be conservative considering that uncertainties in river discharge in tropical
508 regions have been shown to exceed 200 % (Kiang et al., 2018). The mean monthly relative uncertainty
509 for ET_{WB} in most basins appears to be in the same order of magnitude (16 %) with results obtained
510 in the Amazon basin (Baker et al., 2021). Results also showed that the relative uncertainty in ET_{WB}
511 is not influenced by basin size as most basins produced similar (same order of magnitude) uncertainty
512 estimates. The relative uncertainty in monthly ET_{WB} was higher during the rainy season. This can be
513 linked to high rainfall input during the rainy season which translates to high river discharge and
514 TWSC thereby increasing the absolute uncertainties in the different water balance components used
515 in estimating ET_{WB} . Results from this study suggest that the relative the uncertainty in monthly ET_{WB}
516 may be substantial which can potentially influence the performance of ET products when they are
517 evaluated using the ET_{WB} method. We therefore recommend that evaluating the performance of ET
518 products at monthly timescale should be accompanied with the estimataion of relative uncertainties.

519

520 **5. Conclusions**

521 The objectives of this study were to assess the performance of water resources reanalysis and
522 evapotranspiration products and to estimate the relative uncertainties in monthly ET_{WB} across eight
523 basins in Africa. It should be noted the evaluation of the performance of WRR and ET products in
524 this study did not explicitly consider the influence the models structure, parameters and input data on
525 their performance. However, we do acknowledge that these factors could have significant impact on
526 the performance of the different models evaluated in this study.

527 The evaluation of WRR products for discharge simulation show varying strengths and
528 weaknesses for the different models. Some models were able to capture the discharge dynamics in
529 the basins while others could not adequately capture this pattern. Differences in the model
530 performance can be attributed to differences model structure, parameters, input data used in driving
531 the models and the spatial resolution of the WRR products. Apart from Noah which is a land surface
532 model (LSM), global hydrological models (GHMs) performed better than LSMs except
533 PCRGLOBW..

534 Evaluation of gridded ET products also revealed varying strengths and weaknesses for the
535 different products. Based on the different evaluation criteria (bias, RMSE, Pearson correlation
536 coefficient, and temporal ET variability), Noah appears to outperform most of other ET estimates and
537 may therefore be recommended for water security assessment in the region. More so, because of water
538 balance closure and the availability of other water balance components (runoff, soil moisture and
539 baseflow). Our results also suggest that the performance of satellite-based ET products is not
540 influenced by spatial resolution, while differences in ET estimates may be attributed to differences in
541 model structure, parameters and the input data used to drive each ET model. On the contrary, spatial
542 resolution appears to have a significant impact on the performance of WRR in simulating ET
543 estimates.

544 Our results also revealed that the relative uncertainties in monthly ET_{WB} were substantially
545 higher during the rainy season which can be attributed to uncertainties inherent in higher rainfall
546 leading to an increase in discharge magnitude and TWSC during this period. Results also revealed
547 that uncertainty in river discharge is the dominant source of uncertainty in ET_{WB} . This underscores
548 the need to prioritize the installation of new gauging stations while upgrading existing stations. This
549 is because uncertainties in river discharge could constrain the ability to fully understand long-term
550 hydrologic variability and undermine discharge prediction.

551 Results from this study suggest that WRR and ET products may be used for water security
552 assessment in poorly gauged basins. However, it is imperative to evaluate the performance of these
553 products in representative gauged basins before applying them in poorly gauged basins. This is
554 because applying the products in poorly gauged basins without evaluating their performance may

555 lead to poor water management decisions with wider policy and financial implications. However,
556 there is also a need for WRR and ET products to be driven by input data from multiple sources to
557 reduce uncertainties in the input data and at the same time, the spatial resolution of WRR products
558 needs to be enhanced. Results from this study may be used by the products developers to improve on
559 the quality of future generations of WRR and ET products.

560 **Author contributions:** EN and RGB designed the methodological framework and contributed to the
561 entire strategic and conceptual framework of the study. EN prepared the data, performed the analyses,
562 interpreted the results and wrote the original draft. JN and EIB provided discharge data for the Mono
563 and Oueme basins respectively. All authors read the paper and provided feedback.

564 **Competing interests:** The authors declare that they have no conflict of interest.

565 **Acknowledgements:** E.N. was funded by the Leverhulme Trust Early Career Fellowship – Award
566 Number ECF–097–2020. We are grateful to Coralie Adams at Manchester University for writing the
567 Python code that was used to produce Figures 4 & 8.

568 **References**

- 569 Abatzoglou, J. T., Dobrowski, S. Z., Parks, S. A., and Hegewisch, K. C.: TerraClimate, a high-
570 resolution global dataset of monthly climate and climatic water balance from 1958–2015,
571 Scientific data, 5, 1-12, <https://doi.org/10.1038/sdata.2017.191>, 2018.
- 572 Adeyeri, O. E. and Ishola, K. A.: Variability and Trends of Actual Evapotranspiration over West
573 Africa: The Role of Environmental Drivers, Agricultural and Forest Meteorology, 308-309,
574 108574, <https://doi.org/10.1016/j.agrformet.2021.108574>, 2021.
- 575 Andam-Akorful, S. A., Ferreira, V. G., Awange, J. L., Forootan, E., and He, X. F.: Multi-model and
576 multi-sensor estimations of evapotranspiration over the Volta Basin, West Africa,
577 International Journal of Climatology, 35, 3132-3145, <https://doi.org/10.1002/joc.4198>, 2015.
- 578 Baker, J. C., Garcia-Carreras, L., Gloor, M., Marsham, J. H., Buermann, W., da Rocha, H. R., Nobre,
579 A. D., de Araujo, A. C., and Spracklen, D. V.: Evapotranspiration in the Amazon: spatial
580 patterns, seasonality, and recent trends in observations, reanalysis, and climate models,
581 Hydrology and Earth System Sciences, 25, 2279-2300, [https://doi.org/10.5194/hess-25-2279-
582 2021](https://doi.org/10.5194/hess-25-2279-2021), 2021.
- 583 Balsamo, G., Beljaars, A., Scipal, K., Viterbo, P., van den Hurk, B., Hirschi, M., and Betts, A. K.: A
584 revised hydrology for the ECMWF model: Verification from field site to terrestrial water
585 storage and impact in the Integrated Forecast System, Journal of hydrometeorology, 10, 623-
586 643, <https://doi.org/10.1175/2008JHM1068.1>, 2009.
- 587 Biancamaria, S., Mballo, M., Le Moigne, P., Sánchez Pérez, J. M., Espitalier-Noël, G., Grusson, Y.,
588 Cakir, R., Häfliger, V., Barathieu, F., Trasmonte, M., Boone, A., Martin, E., and Sauvage, S.:
589 Total water storage variability from GRACE mission and hydrological models for a 50,000
590 km² temperate watershed: the Garonne River basin (France), Journal of Hydrology: Regional
591 Studies, 24, 100609, <https://doi.org/10.1016/j.ejrh.2019.100609>, 2019.
- 592 Blatchford, M. L., Mannaerts, C. M., Njuki, S. M., Nouri, H., Zeng, Y., Pelgrum, H., Wonink, S., and
593 Karimi, P.: Evaluation of WaPOR V2 evapotranspiration products across Africa,
594 Hydrological processes, 34, 3200-3221, <https://doi.org/10.1002/hyp.13791>, 2020.
- 595 Burnett, M. W., Quetin, G. R., and Konings, A. G.: Data-driven estimates of evapotranspiration and
596 its controls in the Congo Basin, Hydrol. Earth Syst. Sci., 24, 4189-4211,
597 <https://doi.org/10.5194/hess-24-4189-2020>, 2020.

- 598 Byers, E., Gidden, M., Leclère, D., Balkovic, J., Burek, P., Ebi, K., Greve, P., Grey, D., Havlik, P.,
599 and Hillers, A.: Global exposure and vulnerability to multi-sector development and climate
600 change hotspots, *Environmental Research Letters*, 13, 055012, <https://doi.org/10.1088/1748-9326/aabf45>, 2018.
- 602 Couason, A., Eilander, D., Muis, S., Veldkamp, T. I., Haigh, I. D., Wahl, T., Winsemius, H. C., and
603 Ward, P. J.: Measuring compound flood potential from river discharge and storm surge
604 extremes at the global scale, *Natural Hazards and Earth System Sciences*, 20, 489-504,
605 <https://doi.org/10.5194/nhess-20-489-2020>, 2020.
- 606 Decharme, B., Alkama, R., Douville, H., Becker, M., and Cazenave, A.: Global Evaluation of the
607 ISBA-TRIP Continental Hydrological System. Part II: Uncertainties in River Routing
608 Simulation Related to Flow Velocity and Groundwater Storage, *Journal of
609 Hydrometeorology*, 11, 601-617, <https://doi.org/10.1175/2010JHM1212.1>, 2010.
- 610 Dinku, T., Funk, C., Peterson, P., Maidment, R., Tadesse, T., Gadain, H., and Ceccato, P.: Validation
611 of the CHIRPS satellite rainfall estimates over eastern Africa, *Quarterly Journal of the Royal
612 Meteorological Society*, 144, 292-312, <https://doi.org/10.1002/qj.3244>, 2018.
- 613 Flörke, M., Schneider, C., and McDonald, R. I.: Water competition between cities and agriculture
614 driven by climate change and urban growth, *Nature Sustainability*, 1, 51-58,
615 <https://doi.org/10.1038/s41893-017-0006-8>, 2018.
- 616 Funk, C., Peterson, P., Landsfeld, M., Pedreros, D., Verdin, J., Shukla, S., Husak, G., Rowland, J.,
617 Harrison, L., and Hoell, A.: The climate hazards infrared precipitation with stations—a new
618 environmental record for monitoring extremes, *Scientific data*, 2, 1-21, 2015.
- 619 Gründemann, G. J., Werner, M., and Veldkamp, T. I.: The potential of global reanalysis datasets in
620 identifying flood events in Southern Africa, *Hydrology and Earth System Sciences*, 22, 4667-
621 4683, <https://doi.org/10.1038/sdata.2015.66>, 2018.
- 622 Gupta, H. V., Kling, H., Yilmaz, K. K., and Martinez, G. F.: Decomposition of the mean squared
623 error and NSE performance criteria: Implications for improving hydrological modelling,
624 *Journal of Hydrology*, 377, 80-91, <https://doi.org/10.1016/j.jhydrol.2009.08.003>, 2009.
- 625 Harrigan, S., Zsoter, E., Alfieri, L., Prudhomme, C., Salamon, P., Wetterhall, F., Barnard, C., Cloke,
626 H., and Pappenberger, F.: GloFAS-ERA5 operational global river discharge reanalysis 1979–
627 present, *Earth System Science Data*, 12, 2043-2060, <https://doi.org/10.5194/essd-12-2043-2020>, 2020.
- 629 Hirpa, F. A., Alfieri, L., Lees, T., Peng, J., Dyer, E., and Dadson, S. J.: Streamflow response to climate
630 change in the Greater Horn of Africa, *Climatic Change*, 156, 341-363,
631 <https://doi.org/10.1007/s10584-019-02547-x>, 2019.
- 632 Jiang, Y. and Liu, Z.: Evaluations of Remote Sensing-Based Global Evapotranspiration Datasets at
633 Catchment Scale in Mountain Regions, *Remote Sensing*, 13, 5096,
634 <https://doi.org/10.3390/rs13245096>, 2021.
- 635 Jung, H. C., Getirana, A., Arsenault, K. R., Holmes, T. R. H., and McNally, A.: Uncertainties in
636 Evapotranspiration Estimates over West Africa, *Remote Sensing*, 11, 892,
637 <https://doi.org/10.3390/rs11080892>, 2019.
- 638 Kabuya, P. M., Hughes, D. A., Tshimanga, R. M., Trigg, M. A., and Bates, P.: Establishing
639 uncertainty ranges of hydrologic indices across climate and physiographic regions of the
640 Congo River Basin, *Journal of Hydrology: Regional Studies*, 30, 100710,
641 <https://doi.org/10.1016/j.ejrh.2020.100710>, 2020.
- 642 Kamta, F. N., Schilling, J., and Scheffran, J.: Water Resources, Forced Migration and Tensions with
643 Host Communities in the Nigerian Part of the Lake Chad Basin, *Resources*, 10, 27, 2021.
- 644 Kiang, J. E., Gazoorian, C., McMillan, H., Coxon, G., Le Coz, J., Westerberg, I. K., Belleville, A.,
645 Sevrez, D., Sikorska, A. E., Petersen-Øverleir, A., Reitan, T., Freer, J., Renard, B.,
646 Mansanarez, V., and Mason, R.: A Comparison of Methods for Streamflow Uncertainty
647 Estimation, *Water Resources Research*, 54, 7149-7176,
648 <https://doi.org/10.1029/2018WR022708>, 2018.

649 Koukoulou, M., Nikolopoulos, E. I., Dokou, Z., and Anagnostou, E. N.: Evaluation of global water
650 resources reanalysis products in the upper Blue Nile River Basin, *Journal of*
651 *Hydrometeorology*, 21, 935-952, <https://doi.org/10.1175/JHM-D-19-0233.1>, 2020.

652 Krabbenhoft, C. A., Allen, G. H., Lin, P., Godsey, S. E., Allen, D. C., Burrows, R. M., DelVecchia,
653 A. G., Fritz, K. M., Shanafield, M., Burgin, A. J., Zimmer, M. A., Detry, T., Dodds, W. K.,
654 Jones, C. N., Mims, M. C., Franklin, C., Hammond, J. C., Zipper, S., Ward, A. S., Costigan,
655 K. H., Beck, H. E., and Olden, J. D.: Assessing placement bias of the global river gauge
656 network, *Nature Sustainability*, 2022.

657 Krinner, G., Viovy, N., de Noblet-Ducoudré, N., Ogée, J., Polcher, J., Friedlingstein, P., Ciais, P.,
658 Sitch, S., and Prentice, I. C.: A dynamic global vegetation model for studies of the coupled
659 atmosphere-biosphere system, *Global Biogeochemical Cycles*, 19,
660 <https://doi.org/10.1029/2003GB002199>, 2005.

661 Laipelt, L., Kayser, R. H. B., Fleischmann, A. S., Ruhoff, A., Bastiaanssen, W., Erickson, T. A., and
662 Melton, F.: Long-term monitoring of evapotranspiration using the SEBAL algorithm and
663 Google Earth Engine cloud computing, *ISPRS Journal of Photogrammetry and Remote*
664 *Sensing*, 178, 81-96, <https://doi.org/10.1016/j.isprsjprs.2021.05.018>, 2021.

665 Lakew, H. B., Moges, S. A., Anagnostou, E. N., Nikolopoulos, E. I., and Asfaw, D. H.: Evaluation
666 of global water resources reanalysis runoff products for local water resources applications:
667 case study-upper Blue Nile basin of Ethiopia, *Water Resources Management*, 34, 2157-2177,
668 <https://doi.org/10.1007/s11269-019-2190-y>, 2020.

669 Larbi, I., Hountondji, F. C. C., Dotse, S.-Q., Mama, D., Nyamekye, C., Adeyeri, O. E., Djan'na
670 Koubodana, H., Odoom, P. R. E., and Asare, Y. M.: Local climate change projections and
671 impact on the surface hydrology in the Vea catchment, West Africa, *Hydrology Research*, 52,
672 1200-1215, <https://doi.org/10.2166/nh.2021.096>, 2021.

673 Liu, W.: Evaluating remotely sensed monthly evapotranspiration against water balance estimates at
674 basin scale in the Tibetan Plateau, *Hydrology Research*, 49, 1977-1990, 10.2166/nh.2018.008,
675 2018.

676 López, P. L., Sultana, T., Kafi, M. A. H., Hossain, M. S., Khan, A. S., and Masud, M. S.: Evaluation
677 of global water resources reanalysis data for estimating flood events in the Brahmaputra River
678 Basin, *Water Resources Management*, 34, 2201-2220, <https://doi.org/10.1007/s11269-020-02546-z>, 2020.

680 Ma, N., Szilagyi, J., and Zhang, Y.: Calibration-free complementary relationship estimates terrestrial
681 evapotranspiration globally, *Water Resources Research*, 57, e2021WR029691, 2021.

682 Martens, B., Miralles, D. G., Lievens, H., Van Der Schalie, R., De Jeu, R. A., Fernández-Prieto, D.,
683 Beck, H. E., Dorigo, W. A., and Verhoest, N. E.: GLEAM v3: Satellite-based land evaporation
684 and root-zone soil moisture, *Geoscientific Model Development*, 10, 1903-1925,
685 <https://doi.org/10.5194/gmd-10-1903-2017>, 2017.

686 McNally, A., Arsenault, K., Kumar, S., Shukla, S., Peterson, P., Wang, S., Funk, C., Peters-Lidard,
687 C. D., and Verdin, J. P.: A land data assimilation system for sub-Saharan Africa food and
688 water security applications, *Scientific data*, 4, 1-19, 2017.

689 McNamara, I., Baez-Villanueva, O. M., Zomorodian, A., Ayyad, S., Zambrano-Bigiarini, M., Zaroug,
690 M., Mersha, A., Nauditt, A., Mbuliro, M., and Wamala, S.: How well do gridded precipitation
691 and actual evapotranspiration products represent the key water balance components in the
692 Nile Basin?, *Journal of Hydrology: Regional Studies*, 37, 100884,
693 <https://doi.org/10.1016/j.ejrh.2021.100884>, 2021.

694 Moriasi, D., G. Arnold, J., W. Van Liew, M., L. Bingner, R., D. Harmel, R., and L. Veith, T.: Model
695 Evaluation Guidelines for Systematic Quantification of Accuracy in Watershed Simulations,
696 *Transactions of the ASABE*, 50, 885-900, <https://doi.org/10.13031/2013.23153>, 2007.

697 Mu, Q., Zhao, M., and Running, S. W.: Improvements to a MODIS global terrestrial
698 evapotranspiration algorithm, *Remote sensing of environment*, 115, 1781-1800,
699 <https://doi.org/10.1016/j.rse.2011.02.019>, 2011.

700 Mu, Q., Heinsch, F. A., Zhao, M., and Running, S. W.: Development of a global evapotranspiration
701 algorithm based on MODIS and global meteorology data, *Remote sensing of Environment*,
702 111, 519-536, <https://doi.org/10.1016/j.rse.2007.04.015>, 2007.

703 Nagabhatla, N., Cassidy-Neumiller, M., Francine, N. N., and Maatta, N.: Water, conflicts and
704 migration and the role of regional diplomacy: Lake Chad, Congo Basin, and the Mbororo
705 pastoralist, *Environmental Science & Policy*, 122, 35-48,
706 <https://doi.org/10.1016/j.envsci.2021.03.019>, 2021.

707 Neal, J., Schumann, G., Bates, P., Buytaert, W., Matgen, P., and Pappenberger, F.: A data assimilation
708 approach to discharge estimation from space, *Hydrological Processes*, 23, 3641-3649,
709 <https://doi.org/10.1002/hyp.7518>, 2009.

710 Nkiaka, E.: Water security assessment in poorly gauged regions using the water balance and water
711 footprint concepts and satellite observations, *Hydrology Research*,
712 <https://doi.org/10.2166/nh.2022.124>, 2022.

713 Nkiaka, E., Nawaz, N., and Lovett, J.: Using self-organizing maps to infill missing data in hydro-
714 meteorological time series from the Logone catchment, Lake Chad basin, *Environmental*
715 *Monitoring and Assessment*, 188, 1-12, <https://doi.org/10.1007/s10661-016-5385-1>, 2016.

716 Nkiaka, E., Bryant, R. G., Okumah, M., and Gomo, F. F.: Water security in sub-Saharan Africa:
717 Understanding the status of sustainable development goal 6, *WIREs Water*, 8, e1552,
718 <https://doi.org/10.1002/wat2.1552>, 2021.

719 Nkiaka, E., Taylor, A., Dougill, A. J., Antwi-Agyei, P., Adefisan, E. A., Ahiataku, M. A., Baffour-
720 Ata, F., Fournier, N., Indasi, V. S., and Konte, O.: Exploring the need for developing impact-
721 based forecasting in West Africa, *Frontiers in Climate*, 11,
722 <https://doi.org/10.3389/fclim.2020.565500>, 2020.

723 Odusanya, A. E., Mehdi, B., Schürz, C., Oke, A. O., Awokola, O. S., Awomeso, J. A., Adejuwon, J.
724 O., and Schulz, K.: Multi-site calibration and validation of SWAT with satellite-based
725 evapotranspiration in a data-sparse catchment in southwestern Nigeria, *Hydrology and Earth*
726 *System Sciences*, 23, 1113-1144, <https://doi.org/10.5194/hess-23-1113-2019>, 2019.

727 Oussou, F. E., Ndehedehe, C. E., Oloukoi, J., Yalo, N., Boukari, M., and Diaw, A. T.:
728 Characterization of the hydro-geological regime of fractured aquifers in Benin (West-Africa)
729 using multi-satellites and models, *Journal of Hydrology: Regional Studies*, 39, 100987,
730 <https://doi.org/10.1016/j.ejrh.2021.100987>, 2022.

731 Rodell, M., McWilliams, E. B., Famiglietti, J. S., Beaudoin, H. K., and Nigro, J.: Estimating
732 evapotranspiration using an observation based terrestrial water budget, *Hydrological*
733 *Processes*, 25, 4082-4092, <https://doi.org/10.1002/hyp.8369>, 2011.

734 Rodell, M., Houser, P., Jambor, U., Gottschalck, J., Mitchell, K., Meng, C.-J., Arsenault, K.,
735 Cosgrove, B., Radakovich, J., and Bosilovich, M.: The global land data assimilation system,
736 *Bulletin of the American Meteorological society*, 85, 381-394,
737 <https://doi.org/10.1175/BAMS-85-3-381>, 2004.

738 Rodell, M., Beaudoin, H. K., L'Ecuyer, T. S., Olson, W. S., Famiglietti, J. S., Houser, P. R., Adler,
739 R., Bosilovich, M. G., Clayson, C. A., Chambers, D., Clark, E., Fetzer, E. J., Gao, X., Gu, G.,
740 Hilburn, K., Huffman, G. J., Lettenmaier, D. P., Liu, W. T., Robertson, F. R., Schlosser, C.
741 A., Sheffield, J., and Wood, E. F.: The Observed State of the Water Cycle in the Early Twenty-
742 First Century, *Journal of Climate*, 28, 8289-8318, <https://doi.org/10.1175/JCLI-D-14-00555.1>, 2015.

743
744 Rodríguez, E., Sánchez, I., Duque, N., Arboleda, P., Vega, C., Zamora, D., López, P., Kaune, A.,
745 Werner, M., and García, C.: Combined use of local and global hydro meteorological data with
746 hydrological models for water resources management in the Magdalena-Cauca Macro Basin-
747 Colombia, *Water Resources Management*, 34, 2179-2199, 2020.

748 Saha, S., Moorthi, S., Wu, X., Wang, J., Nadiga, S., Tripp, P., Behringer, D., Hou, Y.-T., Chuang,
749 H.-y., and Iredell, M.: The NCEP climate forecast system version 2, *Journal of climate*, 27,
750 2185-2208, <https://doi.org/10.1175/JCLI-D-12-00823.1>, 2014.

751 Satgé, F., Defrance, D., Sultan, B., Bonnet, M.-P., Seyler, F., Rouche, N., Pierron, F., and Paturel, J.-
752 E.: Evaluation of 23 gridded precipitation datasets across West Africa, *Journal of Hydrology*,
753 581, 124412, 2020.

754 Schellekens, J., Dutra, E., Martínez-De La Torre, A., Balsamo, G., Van Dijk, A., Sperna Weiland, F.,
755 Minvielle, M., Calvet, J.-C., Decharme, B., and Eisner, S.: A global water resources ensemble
756 of hydrological models: the earthH2Observe Tier-1 dataset, *Earth System Science Data*, 9, 389-
757 413, 2017.

758 Senay, G. B., Bohms, S., Singh, R. K., Gowda, P. H., Velpuri, N. M., Alemu, H., and Verdin, J. P.:
759 Operational evapotranspiration mapping using remote sensing and weather datasets: A new
760 parameterization for the SSEB approach, *JAWRA Journal of the American Water Resources
761 Association*, 49, 577-591, <https://doi.org/10.1111/jawr.12057>, 2013.

762 Sheffield, J., Wood, E. F., Pan, M., Beck, H., Coccia, G., Serrat-Capdevila, A., and Verbist, K.:
763 Satellite remote sensing for water resources management: Potential for supporting sustainable
764 development in data-poor regions, *Water Resources Research*, 54, 9724-9758, 2018.

765 Shen, Z., Yong, B., Gourley, J. J., Qi, W., Lu, D., Liu, J., Ren, L., Hong, Y., and Zhang, J.: Recent
766 global performance of the Climate Hazards group Infrared Precipitation (CHIRP) with
767 Stations (CHIRPS), *Journal of Hydrology*, 591, 125284,
768 <https://doi.org/10.1016/j.jhydrol.2020.125284>, 2020.

769 Sikder, M., David, C. H., Allen, G. H., Qiao, X., Nelson, E. J., and Matin, M. A.: Evaluation of
770 available global runoff datasets through a river model in support of transboundary water
771 management in South and Southeast Asia, *Frontiers in Environmental Science*, 171,
772 <https://doi.org/10.3389/fenvs.2019.00171>, 2019.

773 Slater, L. J., Anderson, B., Buechel, M., Dadson, S., Han, S., Harrigan, S., Kelder, T., Kowal, K.,
774 Lees, T., and Matthews, T.: Nonstationary weather and water extremes: a review of methods
775 for their detection, attribution, and management, *Hydrology and Earth System Sciences*, 25,
776 3897-3935, <https://doi.org/10.5194/hess-25-3897-2021>, 2021.

777 Smith, M. W., Willis, T., Alfieri, L., James, W. H. M., Trigg, M. A., Yamazaki, D., Hardy, A. J.,
778 Bisselink, B., De Roo, A., Macklin, M. G., and Thomas, C. J.: Incorporating hydrology into
779 climate suitability models changes projections of malaria transmission in Africa, *Nature
780 Communications*, 11, 4353, <https://doi.org/10.1038/s41467-020-18239-5>, 2020.

781 Tapley, B. D., Watkins, M. M., Flechtner, F., Reigber, C., Bettadpur, S., Rodell, M., Sasgen, I.,
782 Famiglietti, J. S., Landerer, F. W., Chambers, D. P., Reager, J. T., Gardner, A. S., Save, H.,
783 Ivins, E. R., Swenson, S. C., Boening, C., Dahle, C., Wiese, D. N., Dobslaw, H., Tamisiea,
784 M. E., and Velicogna, I.: Contributions of GRACE to understanding climate change, *Nature
785 Climate Change*, 9, 358-369, <https://doi.org/10.1038/s41558-019-0456-2>, 2019.

786 Thiemi, V., Bisselink, B., Pappenberger, F., and Thielen, J.: A pan-African medium-range ensemble
787 flood forecast system, *Hydrol. Earth Syst. Sci.*, 19, 3365-3385, [https://doi.org/10.5194/hess-
788 19-3365-2015](https://doi.org/10.5194/hess-19-3365-2015), 2015.

789 UNDESA: United Nations, Department of Economic and Social Affairs, Population Division Prospects, Volume
790 I: Comprehensive Tables (ST/ESA/SER.A/426), 2019.

791 van Beek, L. P. H., Wada, Y., and Bierkens, M. F. P.: Global monthly water stress: 1. Water balance
792 and water availability, *Water Resources Research*, 47,
793 <https://doi.org/10.1029/2010WR009791>, 2011.

794 Van Der Knijff, J. M., Younis, J., and De Roo, A. P. J.: LISFLOOD: a GIS-based distributed model
795 for river basin scale water balance and flood simulation, *International Journal of Geographical
796 Information Science*, 24, 189-212, 10.1080/13658810802549154, 2010.

797 van Dijk, A. I. J. M., Renzullo, L. J., Wada, Y., and Tregoning, P.: A global water cycle reanalysis
798 (2003–2012) merging satellite gravimetry and altimetry observations with a
799 hydrological multi-model ensemble, *Hydrol. Earth Syst. Sci.*, 18, 2955-2973,
800 <https://doi.org/10.5194/hess-18-2955-2014>, 2014.

- 801 Wada, Y., Wisser, D., and Bierkens, M. F. P.: Global modeling of withdrawal, allocation and
802 consumptive use of surface water and groundwater resources, *Earth Syst. Dynam.*, 5, 15-40,
803 <https://doi.org/10.5194/esd-5-15-2014>, 2014.
- 804 Weedon, G. P., Balsamo, G., Bellouin, N., Gomes, S., Best, M. J., and Viterbo, P.: The WFDEI
805 meteorological forcing data set: WATCH Forcing Data methodology applied to ERA-Interim
806 reanalysis data, *Water Resources Research*, 50, 7505-7514,
807 <https://doi.org/10.1002/2014WR015638>, 2014.
- 808 Weerasinghe, I., Bastiaanssen, W., Mul, M., Jia, L., and Van Griensven, A.: Can we trust remote
809 sensing evapotranspiration products over Africa?, *Hydrology and Earth System Sciences*, 24,
810 1565-1586, <https://doi.org/10.5194/hess-24-1565-2020>, 2020.
- 811 Wiese, D. N., Landerer, F. W., and Watkins, M. M.: Quantifying and reducing leakage errors in the
812 JPL RL05M GRACE mascon solution, *Water Resources Research*, 52, 7490-7502,
813 <https://doi.org/10.1002/2016WR019344>, 2016.
- 814 Xie, J., Liu, L., Wang, Y., Xu, Y.-P., and Chen, H.: Changes in actual evapotranspiration and its
815 dominant drivers across the Three-River Source Region of China during 1982–2014,
816 *Hydrology Research*, <https://doi.org/10.2166/nh.2022.076>, 2022.
- 817 Zhang, Y., Kong, D., Gan, R., Chiew, F. H. S., McVicar, T. R., Zhang, Q., and Yang, Y.: Coupled
818 estimation of 500 m and 8-day resolution global evapotranspiration and gross primary
819 production in 2002–2017, *Remote Sensing of Environment*, 222, 165-182,
820 <https://doi.org/10.1016/j.rse.2018.12.031>, 2019.
- 821 Zhang, Y., Peña-Arancibia, J. L., McVicar, T. R., Chiew, F. H., Vaze, J., Liu, C., Lu, X., Zheng, H.,
822 Wang, Y., and Liu, Y. Y.: Multi-decadal trends in global terrestrial evapotranspiration and its
823 components, *Scientific reports*, 6, 1-12, <https://doi.org/10.1038/srep19124>, 2016.

824